ChemInform Abstract: Group (III) Nitrides M[Mg 2 Al 2 N 4] (M: Ca, Sr, Ba, Eu) and Ba[Mg 2 Ga 2 N 4]-Structural Relation and Nontypical Luminescence Properties of Eu 2+ Doped Sam...

ARTICLE *in* CHEMISTRY OF MATERIALS · FEBRUARY 2014

Impact Factor: 8.35 · DOI: 10.1002/chin.201505002

CHEMISTRY OF MATERIALS

Article

pubs.acs.org/cm

Group (III) Nitrides $M[Mg_2Al_2N_4]$ (M = Ca, Sr, Ba, Eu) and $Ba[Mg_2Ga_2N_4]$—Structural Relation and Nontypical Luminescence Properties of Eu^{2+} Doped Samples

Philipp Pust,[§,†] Frauke Hintze,[§,†] Cora Hecht,[‡] Volker Weiler,[‡] Andreas Locher,[†] Daniela Zitnanska,[†] Sascha Harm,[†] Detlef Wiechert,[‡] Peter J. Schmidt,[‡] and Wolfgang Schnick*[,†]

[†]Department of Chemistry, University of Munich (LMU), Butenandtstrasse 5-13, 81377 Munich, Germany

[‡]Philips GmbH Lumileds Development Center Aachen, Philipsstrasse 8, 52068 Aachen, Germany

Supporting Information

ABSTRACT: The isotypic nitridomagnesoaluminates $M[Mg_2Al_2N_4]$ (M = Ca,Sr, Ba,Eu) as well as a novel nitridomagnesogallate $Ba[Mg_2Ga_2N_4]$ have been synthesized by high-temperature reactions in arc-welded tantalum ampules. The crystal structures were solved and refined using single-crystal X-ray diffraction or powder X-ray diffraction data, respectively. All compounds crystallize in the UCr_4C_4-structure type (space group $I4/m$ (no. 87), Z = 2, $Ca[Mg_2Al_2N_4]$: a = 8.0655(11), c = 3.2857(7) Å, $wR2$ = 0.085 $Sr[Mg_2Al_2N_4]$: a = 8.1008(11), c = 3.3269(7) Å, $wR2$ = 0.084; $Eu[Mg_2Al_2N_4]$: a = 8.1539(12), c = 3.3430(7) Å, $wR2$ = 0.033; $Ba[Mg_2Al_2N_4]$: a = 8.2602(9), c = 3.43198(19) Å, wRp = 0.031; $Ba[Mg_2Ga_2N_4]$: a = 8.3654(12), c = 3.4411(7) Å, $wR2$ = 0.031) forming highly condensed anionic networks of disordered $(Al/Mg)N_4$ and $(Ga/Mg)N_4$ units, connected to each other by common edges and corners. The M^{2+} site is centered in *vierer* ring channels along [001] and coordinated in a cuboidal surrounding by N. Eu^{2+} doped samples of $M[Mg_2Al_2N_4]$ (M = Ca,Sr,Ba) exhibit nontypical luminescence properties including trapped exciton emission in the red spectral region. These compounds widen the group of novel red-emitting materials such as $Ca[LiAl_3N_4]:Eu^{2+}$, $Sr[LiAl_3N_4]:Eu^{2+}$, or $Sr[Mg_3SiN_4]:Eu^{2+}$. Therefore, deep discussion of the observed anomalous luminescence is essential to understand the correlations between all these materials, which are fundamental to design narrow band luminescence of Eu^{2+} systems.

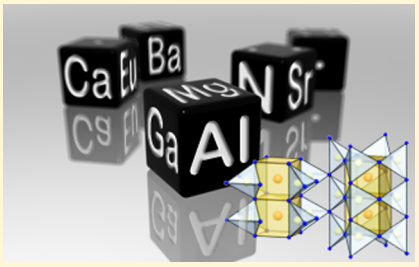

INTRODUCTION

Phosphor-converted light-emitting diodes (pc-LEDs) are expected to be the light sources of the future. As the conversion of electric energy to visible light is much more efficient in pc-LEDs compared to classical light bulbs, the former are expected to be the most relevant candidates for the replacement of energy wasting incandescent light bulbs.[1−4]

Current pc-LED solutions either suffer from lacking intensity in the red spectral region, which limits color rendition properties, or employ red phosphors, which emit a substantial portion of the radiation outside the human eye sensitivity, limiting the luminous efficacy (efficiency weighted by eye sensitivity). The enhancement of both parameters, color rendition (CRI) and luminous efficacy of a white pc-LED, critically depend on the properties (emission maximum and width) of the red-emitting phosphor material.[5] Consequently, in order to improve the efficacy (lm/W), without compromising the CRI, there is a strong demand for novel red emitting phosphor materials with superior luminescence properties.[6,7] Thereby, a number of multinary nitrides of group III and IV elements emerged as attractive host lattices for doping with Eu^{2+}, resulting in interesting luminescence properties. Due to parity allowed $4f^6(^7F)5d^1 \rightarrow 4f^7(^8S_{7/2})$ transitions intense emission can be observed throughout the entire visible spectrum.

Especially the material classes of nitridosilicates, nitridoalumosilicates, and related SiAlONs came into the focus of extensive investigations. In the meantime, several representatives proved to be excellent candidates for application in pc-LEDs.[8]

Recently, a novel group of structurally related phosphor materials was investigated. We could demonstrate that the novel nitridomagnesosilicate $Sr[Mg_3SiN_4]:Eu^{2+}$ represents the most narrow red-emitting Eu^{2+}-doped phosphor material described in literature so far (λ_{em} = 615 nm, fwhm ∼1170 cm^{-1}).[9] The isotypic nitridolithoaluminate $Ca[LiAl_3N_4]:Eu^{2+}$ also exhibits an intense, for a Eu^{2+}-doped material exceptionally narrow, red emission.[10] Both compounds crystallize in the $Na[Li_3SiO_4]$ structure type,[11] which exhibits specific structural features that we believe are beneficial for narrow band red emission. Especially, the ordered and rigid host lattice and the single heavy atom site should be mentioned in this respect.

The isoelectronic compound $Sr[LiAl_3N_4]:Eu^{2+}$, which crystallizes in the $Cs[Na_3PbO_4]$ structure type, could demonstrate the high potential of such materials for industrial application.[12] The employment of such a narrow band red-

Received: June 24, 2014
Revised: August 25, 2014
Published: August 26, 2014

   dx.doi.org/10.1021/cm502280p | Chem. Mater. 2014, 26, 6113−6119

emitting system helps to increase luminous efficacy of a demonstrator pc-LED by 14% (Ra8 = 91, R9 = 57) compared to a commercially available high CRI-LED. Therefore, we started a broadband screening of these as well as related structure types, to obtain new compound classes with adequate luminescence properties and to understand structure−property relations in more detail.

In this contribution, the novel nitridomagnesoaluminates $Ca[Mg_2Al_2N_4]$, $Sr[Mg_2Al_2N_4]$, $Eu[Mg_2Al_2N_4]$, and $Ba[Mg_2Al_2N_4]$ are presented as well as the novel nitridomagnesogallate $Ba[Mg_2Ga_2N_4]$. All five quaternary compounds are isotypic crystallizing in the UCr_4C_4-structure type. Detailed investigations of the crystal structures as well as the nontypical luminescence properties of Eu^{2+} doped samples are reported.

EXPERIMENTAL SECTION

Synthesis. For synthesis of $M[Mg_2Al_2N_4]$ (M = Ca,Sr,Ba,Eu) and $Ba[Mg_2Ga_2N_4]$ different approaches have been employed. All procedures were performed under inert gas atmosphere (Ar) in glove boxes (Unilab, MBraun, Garching; O_2 < 1 ppm, H_2O < 1 ppm).

$Ba[Mg_2Ga_2N_4]$ was synthesized starting from mixtures of the respective metals and NaN_3 as nitrogen source in a sodium melt. Typically, 0.31 mmol NaN_3 (20.1 mg, Acros, 99%), 0.064 mmol Mg (1.53 mg, Alfa Aesar, 99.9%), 0.245 mmol Ga (17.1 mg, Sigma-Aldrich, 99.99%), and 1.95 mmol Na (44.9 mg, Sigma-Aldrich, 99.95%) were used. Furthermore, 0.063 mmol Ba (8.65 mg, Sigma-Aldrich, 99.99%) was added. For luminescence investigations, small amounts of EuF_3 (Sigma-Aldrich 99.95%) were added as dopand. The starting materials were filled into Ta ampules (30 mm length, 10 mm diameter, 0.5 mm wall thickness). The ampules were welded shut under Ar atmosphere and placed in quartz tubes under vacuum to prevent oxidation of the ampules. The respective reaction mixtures were heated to 760 °C in a tube furnace at 50°/h, maintained at that temperature for 48 h, and then cooled to 200 °C at a rate of 3.4°/h. After reaction, the ampules were opened in a glove box and Na was separated from the reaction products by vacuum sublimation at 320 °C for 10 h.

To obtain single crystals of $M[Mg_2Al_2N_4]$ (M = Ca,Sr,Ba,Eu) a faster reaction compared to the above-mentioned metal route was used. Herein, the metal fluorides together with Mg_3N_2 were used. To capture the F^--ions, syntheses were performed in a Li-melt with LiN_3 as the nitrogen source. Typically, 0.3 mmol MF_2 (M = Ca, Sr, Ba; all from Sigma-Aldrich, 99.99%) or EuF_3 (Sigma-Aldrich 99.95%), 0.6 mmol AlF_3 (50.4 mg, Sigma-Aldrich, 99.95%), 0.20 mmol Mg_3N_2 (20.2 mg, Sigma-Aldrich, 99.5%), 0.30 mmol LiN_3 (14.7 mg, synthesized according to Fair et al.),[13] and 3.0 mmol Li (20.8 mg, Sigma-Aldrich, 99.9%) were added. For luminescence investigations of the alkaline-earth compounds, small amounts of EuF_3 were added as dopand. The respective mixtures of starting materials were filled into Ta ampules and sealed in a water-cooled arc-welding device under argon. The ampules were placed in silica tubes and heated in tube furnaces to 900 °C at 200°/h, maintained at that temperature for 24 h, and slowly cooled to 500 °C at a rate of 10°/h. Subsequently, the furnace was turned off and the Ta-ampules were opened under inert gas atmosphere in a glove box.

Bulk samples of $M[Mg_2Al_2N_4]$ (M = Ca,Sr,Ba) were synthesized in a hot isostatic press under nitrogen pressure (7500 PSI) at 1450 °C. Here, stoichiometric mixtures of Mg_3N_2 (Sigma-Aldrich, 99.5%), AlN (Tokuyama, 99%) and MH_2 (M = Sr,Ba; both from Cerac, 99.5%) were used as starting materials.

Electron Microscopy. Electron microscopy was performed on a JEOL JSM 6500 F scanning electron microscope (SEM) equipped with a field emission gun at a maximum acceleration voltage of 30 kV. Synthesized samples were prepared on adhesive conductive carbon pads and coated with a conductive carbon film. The chemical compositions were confirmed by EDX spectroscopy (Oxford Instruments, model 7418), each spectrum recorded on an area limited to one crystal face to avoid influence of possible contaminating phases.

Single-Crystal X-ray Diffraction. The crystal structures of $M[Mg_2Al_2N_4]$ (M = Ca, Sr, Eu) and $Ba[Mg_2Ga_2N_4]$ were determined by single-crystal X-ray diffraction on a Nonius Kappa-CCD diffractometer with graded multilayer X-ray optics and Mo Kα radiation (λ = 0.71073 Å). Absorption correction for $Eu[Mg_2Al_2N_4]$ and $Ba[Mg_2Ga_2N_4]$ was carried out by means of WinGX.[14] The structures were solved by direct methods implemented in SHELXS-97.[15] Crystal structure refinements were carried out with anisotropic displacement parameters for all atoms by full-matrix least-squares calculation on F^2 using SHELXL-97.[15] The corresponding single crystals were prepared in capillaries and checked for quality on a Buerger precession camera.

More details of the structure investigations are available from the Fachinformationszentrum Karlsruhe, D-76344 Eggenstein Leopoldshafen, Germany (Fax: +49 7247 808 666. Email: crysdata@fiz.karlsruhe.de) on quoting the depository numbers CSD-425319 ($Ca[Mg_2Al_2N_4]$), CSD-425321 ($Sr[Mg_2Al_2N_4]$), CSD-425320 ($Eu[Mg_2Al_2N_4]$), CSD-427065 ($Ba[Mg_2Al_2N_4]$), and CSD-425318 ($Ba[Mg_2Ga_2N_4]$).

Powder X-ray Diffraction. Powder X-ray diffraction data were collected on a STOE STADI P diffractometer (Cu Kα_1 radiation, Ge(111) monochromator, position sensitive detector) in Debye−Scherrer geometry or alternatively on a Huber G670 Guinier imaging plate diffractometer (Cu Kα_1 radiation, Ge(111) monochromator). Simulations of Bragg intensities were performed using the WinXPOW program package[16] on the basis of the single-crystal data. Rietveld refinement was carried out using the TOPAS package.[17] The crystal structure of $Ba[Mg_2Al_2N_4]$ was solved and refined from X-ray powder data starting from the crystallographic data of isotypic $Sr[Mg_2Al_2N_4]$.

UV/Vis Spectroscopy. Reflectance spectra were recorded on an Edinburgh Photonics FLS920-s spectrometer with a Xe900 450 W arclamp (Czerny-Turner monochromator with three gratings, single-photon-photomultiplier detector). The spectra were measured between 250 and 780 nm with 5 nm step size.

Luminescence. Luminescence properties of single crystals were investigated using a luminescence microscope consisting of a HORIBA Fluorimax4 Spectrofluorimeter-system, which is attached to an Olympus BX51 microscope via fiber optics. Photoluminescence measurements on powder samples in PTFE sample holders were carried out using an in-house built system based on a 5.3″ integrating sphere and a spectrofluorimeter equipped with a 150 W Xe lamp, two 500 mm Czerny−Turner monochromators, 1800 1/mm lattices, and 250/500 nm lamps, with a spectral range from 230 to 820 nm. Low-temperature emission spectra of powder samples were recorded with an Ocean Optics HR2000 + ES spectrometer (2.048 pixels, grating UA (200−1.100 nm), slit 50) with the samples mounted in a closed-cycle He cryostat.

The excitation wavelength was chosen to 440 nm with a spectral width of 10 nm. The emission spectra were collected in the wavelength interval between 470 and 780 nm with 2 nm step size. Excitation spectra were measured in the wavelength range between 350 and 575 nm (for $M[Mg_2Al_2N_4]:Eu^{2+}$ with M = Ca,Sr) or 615 nm (for $Ba[Mg_2Al_2N_4]:Eu^{2+}$) with 2 nm step size.

RESULTS AND DISCUSSION

Synthesis and Chemical Analysis. With the synthesis methods described above a series of new compounds was obtained, namely $Ca[Mg_2Al_2N_4]$, $Sr[Mg_2Al_2N_4]$, $Ba[Mg_2Al_2N_4]$, $Eu[Mg_2Al_2N_4]$, and $Ba[Mg_2Ga_2N_4]$.

The presented Mg containing nitridoaluminates are to the best of our knowledge the first of their kind. However, since Mg^{2+} and Al^{3+}/Ga^{3+} are both part of the tetrahedral network, classification as nitridomagnesoaluminates and -gallates, according to Hoppe, is more appropriate.[11] All compounds were obtained as rod-shaped crystals. A SEM image of $Sr[Mg_2Al_2N_4]$ is shown exemplarily in Figure 1. Table 1 summarizes the average compositions obtained from EDX-analysis (three measurements on different crystals), normalized according to

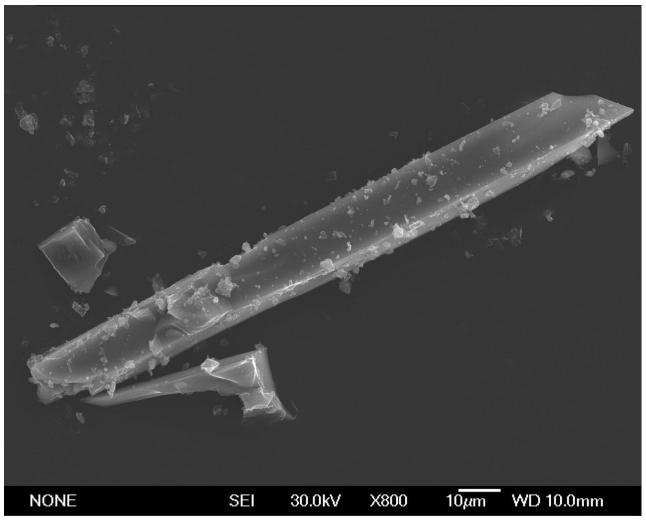

Figure 1. SEM image of rod-shaped $Sr[Mg_2Al_2N_4]$ single crystal.

Table 1. EDX Analyses

EDX analysis	sum formula
$Ca_{1.0}Mg_{1.9}Al_{1.9}N_{4.6}$	$CaMg_2Al_2N_4$
$Sr_{1.0}Mg_{2.0}Al_{2.3}N_{4.6}$	$SrMg_2Al_2N_4$
$Ba_{1.0}Mg_{2.3}Al_{2.0}N_5$	$BaMg_2Al_2N_4$
$Eu_{1.0}Mg_{2.1}Al_{2.1}N_{5.1}$	$EuMg_2Al_2N_4$
$Ba_{1.0}Mg_{2.0}Ga_{2.0}N_{4.7}$	$BaMg_2Ga_2N_4$

the respective heavy atom. All measurements are in good accordance with the expected sum formulas.

As all compounds are isotypic; only $Sr[Mg_2Al_2N_4]$ will be described in the following sections for reasons of clarity. Further crystallographic information on remaining compounds is available in Supporting Information.

Single-Crystal Structure Analysis. The crystal structure of $Sr[Mg_2Al_2N_4]$ was solved and refined in the tetragonal space group $I4/m$ (no. 87) with $a = 8.1008(11)$ and $c = 3.3269(7)$ Å. The crystallographic data of $Sr[Mg_2Al_2N_4]$ are listed in Table 2, the atomic coordinates and displacement parameters are given in Table 3.

$Sr[Mg_2Al_2N_4]$ crystallizes in the UCr_4C_4-structure type[18] forming a three-dimensional network of $(Mg/Al)N_4$-tetrahedra. It is structurally related to the compounds $Ca[LiAl_3N_4]$ and $Sr[LiAl_3N_4]$.[10,12] The framework contains strands of edge-sharing tetrahedra which are connected to each other forming *vierer* rings[19] along [001]. In this network structure, only ammonium-type $N^{[4]}$ atoms connecting four tetrahedral centers (Mg/Al) occur (see Figure 2).

The degree of condensation (i.e., the atomic ratio (Al/Mg):N) in this compound is $\kappa = 1$, corresponding to the value in aluminum nitride AlN. Sr^{2+}-ions are located in every second *vierer*-ring channel, centered in face-sharing cuboidal polyhedra (see Figure 3) with a distance Sr−N of 2.818(2) Å. Compared to the sum of the ionic radii,[20] a slight elongation is observed. An analogous elongation of this distance is also known from all other compounds we report here and was found in $Sr[Mg_2Ga_2N_4]$ (Sr−N: 2.855(2) Å) as well crystallizing in the same structure type.[21] (Mg^{2+}/Al^{3+})-atoms on the tetrahedrally coordinated site are statistically disordered on Wyckoff position 8*h*. The distances (Mg/Al)-N vary between 1.94 and 2.05 Å. Comparable values for Al−N and Mg−N distances appear in the structures of $Sr_3Al_2N_4$ (Al−N: 1.86−1.96 Å) and $CaMg_2N_2$ (Mg−N: 2.13−2.30 Å),[22,23] whereas the reported bond lengths (Mg/Al)−N in $Sr[Mg_2Al_2N_4]$ correspond with the average of these distances.

Table 2. Crystallographic Data of $Sr[Mg_2Al_2N_4]$

formula	$Sr[Mg_2Al_2N_4]$
crystal system	tetragonal
space group	$I4/m$ (no. 87)
lattice params. (Å)	$a = b = 8.1008(11)$ $c = 3.3269(7)$
cell vol. (Å^3)	218.32(6)
formula units/cell	2
$\rho_{calcd.}$ (g·cm^{-3})	3.75
μ (mm^{-1})	12.886
T (K)	293(2)
F(000)	232
diffractometer	κ CCD
radiation (Å), monochromator	Mo Kα (λ = 0.71073), graphite
absorption correction	multiscan
θ range (deg)	3.5−39.2
index ranges	$-14 \le h \le 14$
	$-14 \le k \le 14$
	$-5 \le l \le 5$
independent reflections	365 (R_{int} = 0.0451)
refined params.	16
goodness of fit	1.165
$R1$ (all data); $R1$ ($F^2 > 2\sigma(F^2)$)	0.0313; 0.0309
$wR2$ (all data); $wR2$ ($F^2 > 2\sigma(F^2)$)	0.0838; 0.0834
max/min residual electron density (e·Å^{-3})	1.74/−1.57

Table 3. Atomic Coordinates and Equivalent Isotropic Displacement Parameters (Å^2) of $Sr[Mg_2Al_2N_4]$ and Site Occupancies, Standard Deviations in Parentheses

atom (Wyck.)	x	y	z	U_{eq}	SOF
Sr (2*a*)	0	0	0	0.01357(18)	1
Al (8*h*)	0.18393(14)	0.36311(12)	0	0.0143(2)	0.5
Mg (8*h*)	0.18393(14)	0.36311(12)	0	0.0143(2)	0.5
N (8*h*)	0.4035(4)	0.2370(5)	0	0.0222(6)	1

For the reported Ga containing compound similar results were obtained. Although Ga^{3+} and Mg^{2+} differ significantly in their X-ray scattering intensity no ordering of the atoms on tetrahedral position was observed and the elemental distribution was confirmed by EDX-analysis.

Rietveld refinement of powder-diffraction data validates the structure of $Sr[Mg_2Al_2N_4]$ obtained from single-crystal X-ray diffraction data (see Figure 4 and Supporting Information Table S3). However, besides $Sr[Mg_2Al_2N_4]$ small amounts of AlN can be found as side phase. The insert in Figure 4 shows a comparison of the two most intensive reflections of $M[Mg_2Al_2N_4]$ (M = Ca,Sr,Ba). The ligand field increases from M = Ba to Ca due to a decrease of the lattice constants and shortening of the M−N contacts (see insert Figure 4). Reflectance measurements of nominally undoped powders (see Figure 5) show onsets of the fundamental absorption edge of the host lattices in the 3.65−3.8 eV range.

Luminescence. Eu^{2+}-doped samples of $M[Mg_2Al_2N_4]$ (M = Ca,Sr,Ba) and $Ba[Mg_2Ga_2N_4]$ show a red body color and red luminescence is observed under irradiation with UV to green light. Luminescence investigations were either performed on single crystals in sealed glass capillaries (for $Ba[Mg_2Ga_2N_4]:Eu^{2+}$) or on bulk material on PTFE sample holders.

dx.doi.org/10.1021/cm502280p | *Chem. Mater.* 2014, 26, 6113−6119

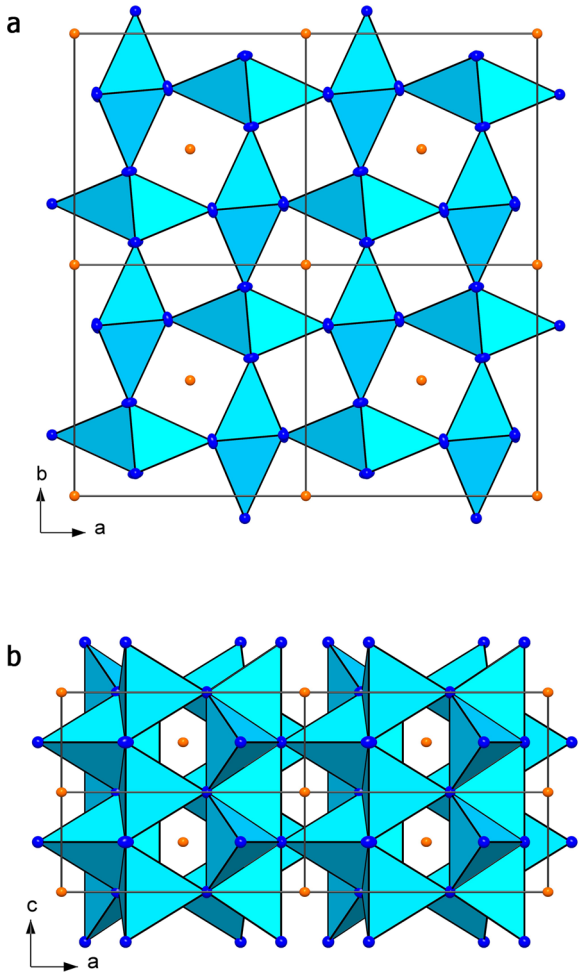

Figure 2. Crystal structure of $Sr[Mg_2Al_2N_4]$. $(Mg/Al)N_4$-tetrahedra blue, nitrogen atoms dark blue, and Sr^{2+}-ions orange. (a) Viewing direction along [001]; (b) viewing direction along [010].

A nominal doping level of 2% $Ba[Mg_2Ga_2N_4]:Eu^{2+}$ yields an emission band peaking at λ_{em} = 649 nm with full width at half-maximum (fwhm) of ~2168 cm^{-1} when excited at 440 nm.

Figure 6 shows excitation, emission and reflectance spectra of $M[Mg_2Al_2N_4]:Eu^{2+}$ (0.1%, M = Ca,Sr,Ba) powder samples. Excitation and reflectance spectra show very similar shapes for all samples with excitation maxima in the 450−480 nm range. The energetic position of the lowest lying absorption band of Eu(II) is estimated to be located at ~540 nm. The strong increase in excitability at wavelengths <350 nm is due to absorption of the host lattice in accordance with the absorption properties of the non doped powders.

The 298 K emission bands show an unusual red shift with increasing alkaline earth atom size with peak positions of λ_{em} = 607 nm (fwhm ~1815 cm^{-1}) for M = Ca, λ_{em} = 612 nm (fwhm ~1823 cm^{-1}) for M = Sr, and λ_{em} = 666 nm (fwhm ~2331 cm^{-1}) for M = Ba. While the emission band shapes are comparable for M = Ca and Sr, the emission of the Ba compound is significantly red-shifted and broadened.

To study these nontypical luminescence properties in more detail, temperature dependent emission measurements were performed for these samples (see Figure 7). Samples for M = Ca and Sr show a significant spectroscopic red-shift of emission at low temperatures. Below ~100 K both compounds show nearly identical spectra peaking at λ_{em} = 625 nm with fwhm = 1715−1785 cm^{-1}. The intensity of emission remains nearly unchanged up to 100 K for both compounds and drops sharply when the temperature is increased (see Figure 8). From 7 to 300 K a peak shift of 474 and 340 cm^{-1} toward higher energies is observed for M = Ca and Sr, respectively. The $Ba[Mg_2Al_2N_4]:Eu^{2+}$(0.1%) sample also shows a red shift of emission at low temperatures (244 cm^{-1} from 300 to 7 K), however, the thermal quenching of the Ba compound emission can be fitted with a single activation energy ($I_T/I_0 = [1 + G\cdot\exp(-E_a/kT)]^{-1}$) (see Figure 8) with E_a = 2022 cm^{-1} (0.25 eV) while the thermal quenching behavior of compounds $M[Mg_2Al_2N_4]:Eu^{2+}$ (0.1%, M = Ca,Sr) points toward a more complex process.

The nontypical emission red-shift within the isotypic series $M[Mg_2Al_2N_4]:Eu^{2+}$ (M = Ca,Sr,Ba) with increasing alkaline earth cation size and the low temperature luminescence properties point toward anomalous luminescence phenomena for these compounds. Large Stokes shifts and nontypical emission red shifts at low temperatures have been observed frequently when Eu(II) 5d levels are located close to the bottom of the host lattice conduction band leading to trapped excition emission.[24] We therefore conclude that normal Eu(II) emission from the $4f^6\ 5d^1$ state is only observed for M = Ca and Sr at high temperatures while at low temperatures (T > 100 K) and for M = Ba emission from a trapped exciton state is being observed.

Figure 9 shows configurational coordinate diagrams for Eu(II) in $M[Mg_2Al_2N_4]:Eu^{2+}$ (M = Sr and Ba) obtained by fitting the experimental data with a basic model assuming linear vibronic coupling.[25] Positions of the lowest lying absorption bands are nearly identical for both compounds and are located at ~540 nm. The rather high phonon frequencies in the 400−500 cm^{-1} range correspond well with the observed small emission band broadening with temperature.[26] For M = Ca and Sr emission most likely originates from a trapped exciton state (orange potential curve in Figure 9) at low temperatures while at higher temperatures the $4f^6\ 5d^1$ state is being thermally populated and normal emission at higher energies is observed. A similar luminescence mechanism was observed recently for $Sr_4Al_{14}O_{25}:Eu^{2+}$.[27] For M = Ba the large Stokes shift and large spectral width of emission points toward trapped exciton emission taking place over the complete temperature range. It is likely that the cuboidal coordination of Eu in the title compounds and the long contact lengths for M = Ba stabilizes a trapped exciton state as a comparison with the series of isotypic compounds $MF_2:Eu^{2+}$ (M = Ca,Sr,Ba) suggests.[24] At room temperature the quantum efficiency of a powder layer of $Sr[Mg_2Al_2N_4]:Eu^{2+}$ is in the range of 18% for 440 nm excitation.

With respect to the emission maximum and the fwhm the luminescence properties of $M[Mg_2Al_2N_4]:Eu^{2+}$ (M = Ca,Sr,Ba) and $Ba[Mg_2Ga_2N_4]:Eu^{2+}$ are comparable to other red emitting compounds reported in literature, e.g., $Ba_3Ga_3N_5:Eu^{2+}$ (ca. 2 mol% Eu; λ_{em} = 638 nm; fwhm ~2123 cm^{-1}),[28] $(Sr,Ba)_2Si_5N_8:Eu^{2+}$ (λ_{em} = 590−625 nm; fwhm ~2050−2600 cm^{-1}),[29] or $(Ca,Sr)AlSiN_3:Eu^{2+}$ (λ_{em} = 610−660 nm; fwhm ~2100−2500 cm^{-1}).[30,31]

The relatively broad emission band of compounds in the UCr_4C_4 structure type results most likely from disordering of the framework cations (here: Mg^{2+} and Al^{3+}). In this case, statistical distribution leads to constantly varying distances (Al^{3+}/Mg^{2+})−N in the tetrahedrally coordinated positions, accompanied by a broad range of Eu−N bond lengths and

dx.doi.org/10.1021/cm502280p | Chem. Mater. 2014, 26, 6113−6119

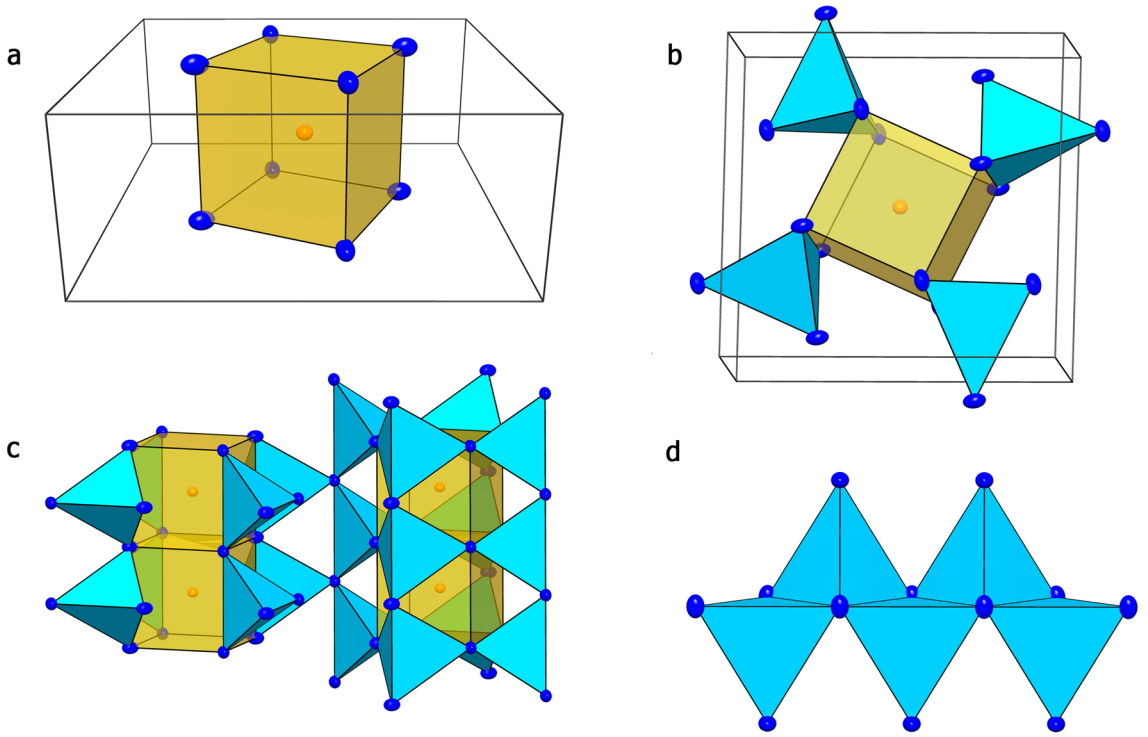

Figure 3. Structural details of $Sr[Mg_2Al_2N_4]$; all atoms are shown as ellipsoids with 50% probability. (a) Cuboid-like coordination of Sr^{2+} (orange) by nitrogen atoms (blue); (b) coordination of the Sr^{2+} centered polyhedra by $(Mg/Al)N_4$-tetrahedra (blue); (c) structure assembly and conjunction of $(Mg/Al)N_4$-tetrahedra (blue); (d) edge sharing of $(Mg/Al)N_4$-tetrahedra strands (blue).

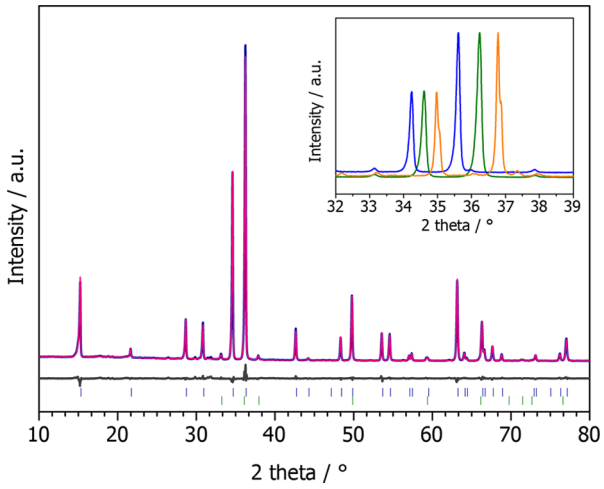

Figure 4. Rietveld refinement (Rp = 0.0305, wRp = 0.0407; 14384 data points) of X-ray powder-diffraction pattern of $Sr[Mg_2Al_2N_4]$ with measured histogram (blue line), calculated pattern (red line), difference curve (gray line), and positions of reflections (blue bars). Positions of AlN reflections (~10 wt%, green bars). Insert: Comparison of the two most intensive reflections of $Ca[Mg_2Al_2N_4]$ orange, $Sr[Mg_2Al_2N_4]$ green, and $Ba[Mg_2Al_2N_4]$ blue.

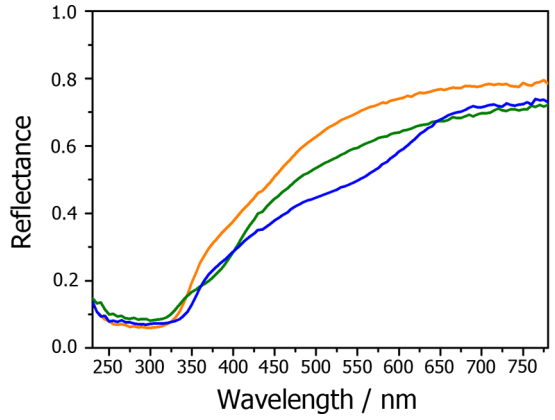

Figure 5. Reflectance spectra for nondoped powders of $Ca[Mg_2Al_2N_4]$ orange, $Sr[Mg_2Al_2N_4]$ green, and $Ba[Mg_2Al_2N_4]$ blue.

environments. The differing crystal fields directly cause inhomogeneous line broadening of the emission band. A similar behavior has been reported for, e.g., $(Ca,Sr)AlSiN_3:Eu^{2+}$, a material that also shows a statistical distribution of the host lattice cations Al and Si that occupy the same crystallographic site.[29] The very narrow emission profiles of ordered variants of the UCr_4C_4 structure type such as $Ca[LiAl_3N_4]:Eu^{2+}$ (ca. 5 mol % Eu; λ_{em} = 668 nm; fwhm of ~1333 cm^{-1}), $Sr[LiAl_3N_4]:Eu^{2+}$ (ca. 0.4 mol % Eu; λ_{em} = 650 nm; fwhm of ~1180 cm^{-1}), or $Sr[Mg_3SiN_4]:Eu^{2+}$ (ca. 2 mol % Eu; λ_{em} = 615 nm; fwhm of ~1170 cm^{-1}) corroborate this assumption.[9,10,12]

CONCLUSIONS

In this contribution, we present the first nitridomagnesoaluminates and a novel nitridomagnesogallate. DiSalvo et al. described the substitutability of Ga^{3+} and Ge^{4+} by Mg^{2+} in nitridogallates and germanates, demonstrated by the two compounds $Sr[Mg_2Ga_2N_4]$ and $Sr[Mg_3GeN_4]$ both crystallizing in the UCr_4C_4-structure type.[21] Back then, this structure type was already discussed as attractive host lattice for luminescent materials, due to the highly symmetric cuboid-like coordination of the heavy atom site. Furthermore, Hoppe et al. could demonstrate the large structural variety of this aristotype by characterizing various ordered oxidic structure types, for example, $Na[Li_3SiO_4]$.[11] Based on this work, we

dx.doi.org/10.1021/cm502280p | Chem. Mater. 2014, 26, 6113−6119

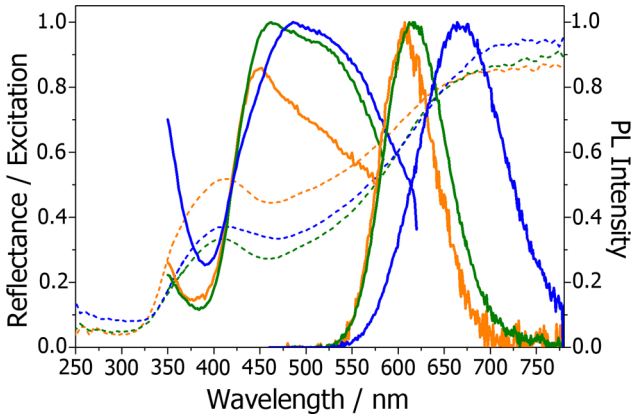

Figure 6. Excitation, reflectance (dashed curves), and emission (λ_{exc} = 440 nm spectra of $M[Mg_2Al_2N_4]:Eu^{2+}$(0.1%) (M = Ca,Sr,Ba) bulk samples at room temperature. $Ca[Mg_2Al_2N_4]:Eu^{2+}$ orange, $Sr[Mg_2Al_2N_4]:Eu^{2+}$ green, and $Ba[Mg_2Al_2N_4]:Eu^{2+}$ blue.

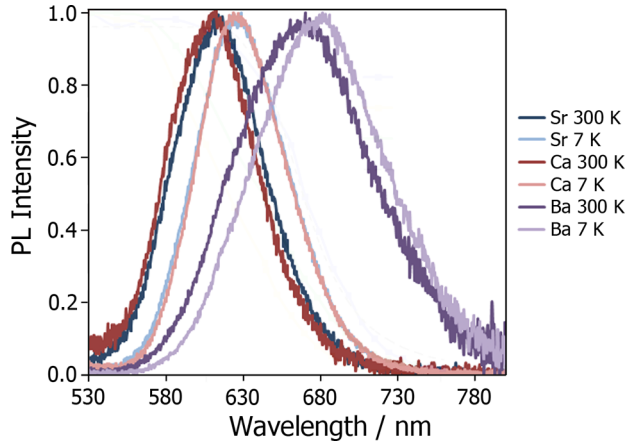

Figure 7. Normalized emission spectra for T = 300 K and T = 7 K of $M[Mg_2Al_2N_4]:Eu^{2+}$:Eu^{2+} (0.1%, M = Ca,Sr,Ba). The figure legend gives information about the assignment of the curves depending on M and the respective temperature.

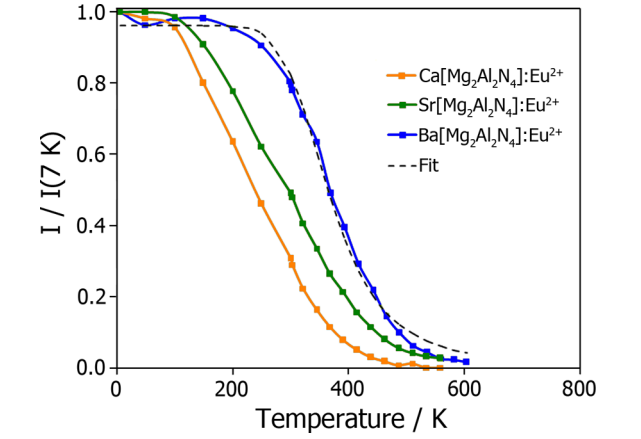

Figure 8. Temperature dependence of emission intensity of $M[Mg_2Al_2N_4]:Eu^{2+}$ (0.1%) (M = Ca,Sr,Ba).

started to develop different substitutional variants based on $AB_2C_2X_4$ and ABC_3X_4 structures either containing Ga/Mg, Al/Mg, Li/Al, or Mg/Si on the tetrahedrally coordinated sites. However, deriving a principle for structural prediction in these systems is quite demanding.

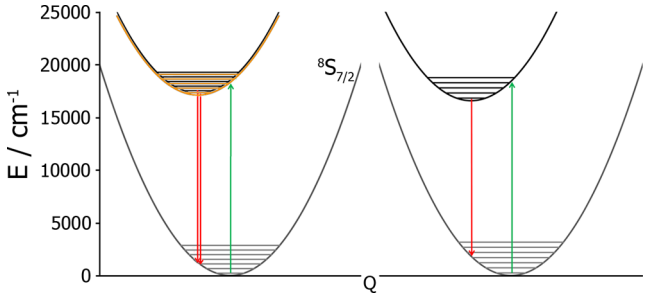

Figure 9. Configurational coordinate diagrams of Eu(II) in $M[Mg_2Al_2N_4]:Eu^{2+}$ (M = Ca,Sr,Ba). Left: M = Sr. The orange potential curve represents a trapped exciton state leading to red-shifted emission at low T for M = Ca, Sr ($\hbar\omega$ = 440 cm^{-1}, S = 2.8, U_0 = 577 nm). Right: M = Ba. The large Stokes shift indicates trapped excition emission being visible over the whole T range ($\hbar\omega$ = 486 cm^{-1}, S = 3.77, U_0 = 603 nm).

All compounds presented in this contribution are isostructural crystallizing in the UCr_4C_4-type with statistical distribution of the tetrahedral network cations Al/Mg or Ga/Mg, respectively. Furthermore, we could show that by employing metal fluorides in combination with Li-melts a number of quaternary compounds is accessible at moderate temperatures up to 900 °C. The presented compounds reveal interesting luminescence properties with emission maxima in the red spectral region and attractive fwhm values.

The nontypical emission red-shift within the isotypic $M[Mg_2Al_2N_4]:Eu^{2+}$ (M = Ca,Sr,Ba) compounds with increasing alkaline earth cation size and the low temperature luminescence properties give strong evidence for anomalous luminescence phenomena. Similar behavior has often been observed when Eu(II) 5d levels are being located close to the bottom of the host lattice conduction band leading to trapped excition emission.[24] Based on our results we conclude that a regular Eu^{2+} emission is only observed for $M[Mg_2Al_2N_4]:Eu^{2+}$ (M = Ca,Sr) at temperatures above 100 K. Below this temperature and also for M = Ba, emission from a trapped exciton state is observed.

These compounds widen the group of novel red-emitting systems like $Ca[LiAl_3N_4]:Eu^{2+}$, $Sr[LiAl_3N_4]:Eu^{2+}$, or $Sr[Mg_3SiN_4]:Eu^{2+}$[9,10,12] and are fundamental to completely understand the mechanisms responsible for narrow band luminescence of Eu^{2+} systems.

■ ASSOCIATED CONTENT

Ⓢ Supporting Information

X-ray crystallographic information files (CIF) of all structures; crystallographic data from single-crystal and powder X-ray diffraction measurements. This material is available free of charge via the Internet at http://pubs.acs.org.

■ AUTHOR INFORMATION

Corresponding Author

*Email: wolfgang.schnick@uni-muenchen.de.

Author Contributions

§P.P. and F.H. contributed equally.

Notes

The authors declare no competing financial interest.

■ ACKNOWLEDGMENTS

The authors gratefully acknowledge financial support the Fonds der Chemischen Industrie (FCI). We also thank Dr. Peter Mayer for single-crystal X-ray data collection, Christian Minke for EDX/SEM investigations (all LMU Munich) as well as Petra Huppertz for single-crystal luminescence measurements and Henning Ohland for UV/vis spectroscopy (both Lumileds Development Center Aachen).

■ REFERENCES

(1) Lin, C. C.; Liu, R.-S. *J. Phys. Chem. Lett.* **2011**, *2*, 1268.
(2) Mikami, M.; Watanabe, H.; Uheda, K.; Shimooka, S.; Shimomura, Y.; Kurushima, T.; Kijima, N. *IOP Conf. Ser.: Mater. Sci. Eng.* **2009**, *1*, 012002.
(3) Mueller-Mach, R.; Mueller, G.; Krames, M. R.; Höppe, H. A.; Stadler, F.; Schnick, W.; Juestel, T.; Schmidt, P. *Phys. Status Solidi A* **2005**, *202*, 1727.
(4) Ye, S.; Xiao, F.; Pan, Y. X.; Ma, Y. Y.; Zhang, Q. Y. *Mater. Sci. Eng. R.* **2010**, *71*, 1.
(5) Krames, M.; Mueller, G. O.; Mueller-Mach, R. B.; Bechtel, H.; Schmidt, P. J. *Wavelength conversion for producing white light from a high power blue light emitting diode (LED)*. PCT Int. Appl. No. WO 2010131133, A1, 2010.
(6) Setlur, A. A. *Electrochem. Soc. Interface* **2009**, *18*, 32.
(7) Xie, R.-J.; Hirosaki, N.; Takeda, T.; Suehiro, T. *ECS J. Solid State Sci. Technol.* **2013**, *2*, R3031.
(8) Zeuner, M.; Pagano, S.; Schnick, W. *Angew. Chem., Int. Ed.* **2011**, *50*, 7754.
(9) Schmiechen, S.; Schneider, H.; Wagatha, P.; Hecht, C.; Schmidt, P. J.; Schnick, W. *Chem. Mater.* **2014**, *26*, 2712.
(10) Pust, P.; Wochnik, A. S.; Baumann, E.; Schmidt, P. J.; Wiechert, D.; Scheu, C.; Schnick, W. *Chem. Mater.* **2014**, *26*, 3544.
(11) Nowitzki, B.; Hoppe, R. *Rev. Chim. Miner.* **1986**, *23*, 217.
(12) Pust, P.; Weiler, V.; Hecht, C.; Tücks, A.; Wochnik, A. S.; Henß, A.-K.; Wiechert, D.; Scheu, C.; Schmidt, P. J.; Schnick, W. *Nat. Mater.* **2014**, *13*, 891.
(13) Fair, H. D.; Walker, R. F. *Energetic Materials 1, Physics and Chemistry of the Inorganic Azides*; Springer: New York/London, 1977.
(14) Farrugia, L. J. *J. Appl. Crystallogr.* **1999**, *32*, 837.
(15) Sheldrick, G. M. *Acta Crystallogr., Sect. A: Found. Crystallogr.* **2008**, *64*, 112.
(16) *WINXPOW—Program for Powder Data Handling*, v2.21; Stoe & Cie GmbH: Darmstadt, Germany, 2007.
(17) Coelho, A. *TOPAS − Academic*, 2007, Coelho Software, Brisbane.
(18) Akselrud, L. G.; Bodak, O. I.; Marusin, E. P. *Sov. Phys. Crystallogr. (Engl. Transl.)* **1989**, *34*, 289.
(19) Liebau established the terms *zweier, dreier, vierer, fünfer* rings. Thereby, a *vierer* ring can be described as four polyhedra connected to each other by common corners forming a ring. The terms derive from the German numerals *drei* (3), *vier* (4), etc. by adding the suffixing ″er″ to the numeral; Liebau, F. *Structural chemistry of silicates*; Springer: Berlin, 1985.
(20) Shannon, R. D. *Acta Crystallogr. Sect. A: Found. Crystallogr.* **1976**, *32*, 751.
(21) Park, D. G.; Dong, Y.; DiSalvo, F. J. *Solid State Sci.* **2008**, *10*, 1846.
(22) Blase, W.; Cordier, G.; Ludwig, M.; Kniep, R. *Z. Naturforsch. B: Chem. Sci.* **1994**, *49*, 501.
(23) Schultz-Coulon, V.; Schnick, W. *Z. Naturforsch. B* **1995**, *50*, 619.
(24) Dorenbos, P. *J. Phys.: Condens. Matter* **2003**, *15*, 2645.
(25) Nazarow, M.; Tsukerblat, B.; Noh, D. Y. *J. Phys. Chem. Solids* **2008**, *69*, 2605.
(26) Curie, D. *Absorption and emission spectra, in: Di Bartolo, Optical Properties of Ions in Solids*; Plenum Press: New York, 1975.
(27) Dutczak, D.; Ronda, C.; Juestel, T.; Meijerink, A. *J. Phys. Chem. A* **2014**, *118*, 1617.
(28) Hintze, F.; Hummel, F.; Schmidt, P. J.; Wiechert, D.; Schnick, W. *Chem. Mater.* **2012**, *24*, 402.
(29) Zeuner, M.; Schmidt, P. J.; Schnick, W. *Chem. Mater.* **2009**, *21*, 2467.
(30) Uheda, K.; Hirosaki, N.; Yamamoto, H. *Phys. Stat. Sol. A* **2006**, *11*, 2712.
(31) Uheda, K.; Hirosaki, N.; Yamamoto, Y.; Naita, A.; Nakajima, T.; Yamamoto, H. *Electrochem. Solid State Lett.* **2006**, *9*, H22.